RESEARCH ARTICLE





Enhanced filtration performance using feed-and-bleed configuration for purification of antibody precipitates

Zhao Li¹ | Ting-Hsi Chen¹ | Erha Andini¹ | Jonathan L Coffman² | Todd Przybycien³ | Andrew L. Zydney¹

Correspondence

Andrew L. Zydney, Department of Chemical Engineering, The Pennsylvania State University, University Park, PA 16802. Email: zydney@engr.psu.edu

Funding information

Division of Chemical, Bioengineering, Environmental, and Transport Systems, Grant/ Award Number: 1705642

Abstract

Precipitation can be used for the initial purification of monoclonal antibodies (mAbs), with the soluble host cell proteins removed in the permeate by tangential flow microfiltration. The objective of this study was to examine the use of a feed-and-bleed configuration to increase the effective conversion (ratio of permeate to feed flow rates) in the hollow fiber module to enable more effective washing of the precipitate. Experiments were performed using human serum Immunoglobulin G (IgG) precipitates formed with 10 mM zinc chloride and 7 wt% polyethylene glycol. The critical flux was evaluated as a function of the shear rate and IgG concentration, with the resulting correlation used to predict conditions that can achieve 90% conversion in a single pass with minimal fouling. Experimental data for both the start-up and steady-state performance are in good agreement with model calculations. These results were used to analyze the performance of an enhanced continuous precipitation–microfiltration process using the feed-and-bleed configuration for the initial capture / purification of a mAb product.

KEYWORDS

antibody, continuous processing, feed and bleed, microfiltration, precipitation

1 | INTRODUCTION

Precipitation is one of the earliest techniques used for large-scale protein purification. Plasma proteins are still purified by precipitation using a combination of ethanol, salt, pH, and temperature to control the selectivity of the precipitation process. There is also growing interest in the use of precipitation for the initial purification (capture) of monoclonal antibody (mAb) products due to the significant increase in product titer that have been achieved over the past two decades. AmAbs have been successfully precipitated using cold ethanol and CaCl₂, polyethylene glycol (PEG), PEG and CaCl₂, CaCl₂ and caprylic acid, PEG and low pH9, zinc chloride (ZnCl₂) and PEG, and elastin-like polypeptides (ELP)^{11,12} among others.

Soluble impurities can be removed from the precipitated protein using a wash step, with the solid-liquid separation accomplished using either centrifugation or membrane microfiltration (MF). Although

centrifugation is the most attractive option for washing of precipitates at small scale, the dense packing of the precipitate / flocs can create challenges in both product recovery and washing in large-scale biomanufacturing. 9 For example, Haller and Kulozik 13 observed significant particle breakdown during continuous centrifugation of α -lactalbumin, with the adhesiveness of the concentrated precipitate leading to high yield loss during discharge from the centrifuge. These problems can be largely eliminated using MF. Hammerschmidt et al. 9 used hollow fiber MF membranes to recover a precipitated mAb, with good performance obtained at a permeate flux of 75 Lm⁻²h⁻¹ using a feed flux of $675 \, \mathrm{Lm^{-2}h^{-1}}$. Good impurity removal was obtained by performing a batch diafiltration with continued recirculation of the precipitate through the membrane module during the wash stage. A similar batch diafiltration was used by Toro-Sierra et al.¹⁴ for the purification of α -lactalbumin by selective precipitation from whey protein isolate.

¹Department of Chemical Engineering, The Pennsylvania State University, University Park, Pennsylvania

²BioProcess Technologies and Engineering, AstraZeneca, Gaithersburg, Maryland

³Department of Chemical & Biological Engineering, Rensselaer Polytechnic Institute, Troy, New York

Although traditional diafiltration can provide high degrees of impurity removal in batch processes, this approach is not readily extendable to continuous processing, which is increasingly attractive for large-scale biomanufacturing.¹⁵ Instead, a countercurrent staged membrane process can be used to achieve the desired degree of washing.^{16,17} The extent of impurity removal (*R*) in this type of multistage countercurrent membrane process is given as¹⁸:

$$R = \frac{C_{\text{feed}}}{C} = \frac{\alpha^{N+1} - 1}{\alpha - 1},\tag{1}$$

with

$$\alpha = \frac{Q_{\text{wash}}}{Q_{\text{food}}} = \frac{x}{1 - x},\tag{2}$$

where C_{feed} is the concentration of soluble impurities in the feed entering the wash step, C is the concentration of soluble impurities leaving the wash step, Q_{feed} is the feed flow rate, Q_{wash} is the flow rate of the wash buffer, N is the number of stages, and x is the conversion in the membrane module (equal to the ratio of the permeate flow rate to inlet feed flow rate for the membrane module). Equations (1) and (2) were developed based on three assumptions concerning the biophysical behavior of the soluble impurities: there is no precipitation of the impurities, there is negligible association of impurities with the precipitate phase or the membrane during the washing, and the impurities are small enough to have sieving coefficient equal to one (negligible retention). The use of large pore size MF membranes to retain precipitate particles, which are typically tens of micrometers in diameter or larger, facilitates good solute transmission. Careful screening and selection of wash solution conditions can mitigate solute adsorptive phenomena. Solute inclusion is managed by forming compact, high fractal dimension particles during the precipitation step.

Li et al. ¹⁸ demonstrated the viability of the countercurrent staged membrane approach for recovery of a mAb from harvested cell culture fluid (HCCF), but they were only able to achieve a 10-fold reduction in host cell protein (HCP) concentration using a two-stage membrane process because of the relatively low conversion in the hollow fiber membrane modules. Note that a 100-fold reduction during a two-stage wash step can be achieved using α = 9.5, which corresponds to more than 90% conversion (x) in the MF module. This is much larger than the conversion achieved by Hammerschmidt et al. x0 (x1) (x2) (x3) or Li et al. x3 (x3) in their MF systems.

One approach that can be used to increase the conversion in a membrane system is to use a feed-and-bleed configuration in which a portion of the retentate stream is recycled back to the feed to significantly increase the flow rate at the entrance to the module. This type of feed-and-bleed operation has been widely employed in the beverage industry, ¹⁹ in water treatment, ²⁰ and in nuclear energy applications. ²¹ Burgstaller et al. ²² and Dutra et al. ²³ used a modified feed-and-bleed system in their studies of mAb precipitation, with the retentate recycled back to a holding tank instead of directly to the hollow fiber module. This system did provide an effective conversion

of 90%, but the large hold-up volume in the system resulted in very long-time lags (more than 6 hr), which would significantly complicate the application of this system in continuous bioprocessing.

The objective of this study was to investigate the use of a feed-and-bleed configuration for increasing the performance of a hollow fiber membrane module used for tangential flow MF to attain the high conversion required for the design of an effective wash step. Experiments were performed using human serum immunoglobulin G (IgG) as a model anti-body with 0.2 μ m pore size mixed cellulose ester hollow fiber membranes. IgG precipitates with >99% yield were produced using a combination of ZnCl₂ and PEG as the precipitants. Correlations were first developed for the critical flux as a function of the shear rate and precipitate concentration, enabling the design of a MF step that can achieve the required conversion for precipitate dewatering and washing with minimal fouling.

2 | MATERIALS AND METHODS

2.1 | Serum IgG

Human serum IgG (NovaBiologics, Oceanside, CA) was used as a model protein; there is considerable interest in IgG precipitation for plasma fractionation and IgG is also a low-cost model for mAb products. The IgG was dissolved in a 50 mM 3-(N-morpholino)propanesulfonic acid (MOPS) buffer at pH 7.0 \pm 0.1 at a total protein concentration of approximately 50 g/L. The IgG was centrifuged at 4800 g for half an hour and then filtered through 0.2 μm polyethersulfone membranes (MilliporeSigma, Burlington, MA) to remove any aggregated/undissolved protein prior to use.

2.2 | Precipitation conditions

Previous work has demonstrated that a combination of a cross-linking agent (ZnCl₂) and a volume exclusion agent (e.g., PEG) can provide very effective precipitation of mAbs. ^{18,22,24,25} Based on these results, all precipitations were performed with 10 mM ZnCl₂, obtained by dilution of a 100 mM solution from Sigma-Aldrich (St. Louis, MO) and 7 wt% PEG (molecular weight of 3,350 g/mol, Sigma-Aldrich); note that all reported concentrations are based on the final solution volume after addition of both precipitants. IgG yield after precipitation was determined by centrifugation of a 1 ml sample of the precipitate at 8,000 rpm for 10 min using a MiniSpin centrifuge (Eppendorf, Hamburg, Germany), with the UV absorbance of the supernatant phase evaluated at 280 nm using an Infinite® m200 Pro microplate reader (Tecan Trading AG, Switzerland). IgG concentrations were determined by comparison of the absorbance at 280 nm to a calibration curve constructed using known standards.

2.3 | Continuous precipitation

Continuous precipitation was conducted using the same experimental system described by Li et al. 18 and shown schematically in Figure 1.

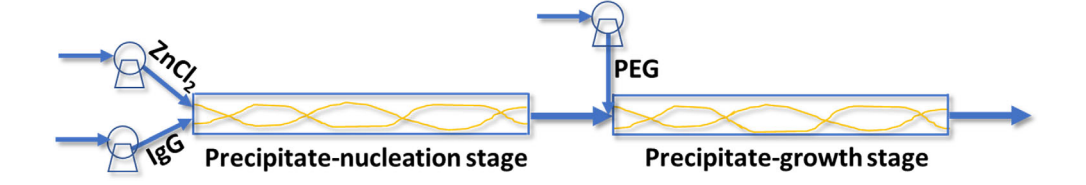
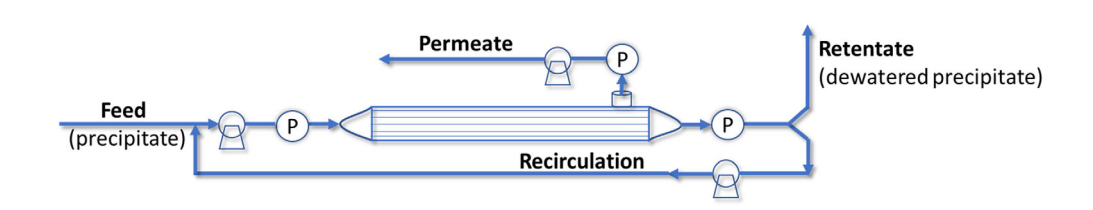


FIGURE 2 Schematic of the feed and bleed configuration



The tubular precipitation reactor was constructed from Tygon® E-LFL tubing (Model 06440–25, Cole-Parmer, Vernon Hills, IL) with inner diameter of 0.48 cm = 3/16 in. fitted with a static-mixer (Koflo Corporation, Cary, IL). The diluted IgG solution was continuously fed to the static mixer at a flow rate of 5 ml/min through a Y-shaped connector with barbed hose fittings using a peristaltic pump (Masterflex L/S, Cole-Parmer). A 100 mM ZnCl $_2$ solution at 1 ml/min was mixed with the IgG solution at the Y-connector to initiate precipitate nucleation, with a 17.5 wt% PEG added as a volume exclusion agent between the first and second static mixers to facilitate the growth of the precipitates. The total residence time in the two-stage precipitation was approximately 30 s. IgG precipitates with a range of concentrations were made by adjusting the IgG concentration in the feed with all other parameters kept constant.

The entire system was flushed and degassed with DI water obtained from a Direct-Q 3 UV-R Water Purification System (EMD Millipore, Billerica, MA), with the pumps calibrated by measuring the water flow rate using timed collection. The precipitation was started by switching the feed to the IgG solution and simultaneously starting the flow of the ZnCl₂ and PEG solutions. The system was allowed to equilibrate for approximately 10 min after initiation of the precipitation.

2.4 | Feed and bleed configuration

The collected IgG precipitates from the continuous precipitation reactor were pumped directly into a 105 cm² MidiKros® hollow fiber membrane module containing 0.2 μm mixed cellulose ester hollow fibers with 0.63 mm ID (Repligen Corporation, Rancho Dominguez, CA). Unlike the typical single-pass mode in tangential flow microfiltration (TFF), a recirculation loop was added to the hollow fiber module as shown in Figure 2. Part of the concentrated retentate stream leaving the module was recirculated back to the feed line using an additional peristaltic pump (Cole-Parmer). Fresh IgG precipitates were mixed with the recycle stream and then fed to the module. The filtrate flux was controlled by a separate peristaltic pump placed on the permeate exit line, with the axial pressure drop (ΔP) and the transmembrane pressure (TMP) monitored using digital pressure gauges

(Ashcroft, Stratford, CT) placed immediately before and after the inlet/outlet ports on both the feed and permeate lines.

The membrane modules and tubing were flushed with DI water and the permeability of the hollow fiber membrane was evaluated to confirm filter integrity. The pumps were then shut off and the feed switched to the precipitated IgG. The feed pump was turned on first, with the recirculation pump started after visual detection of IgG precipitates in the retentate exit line. The permeate pump was started after the recirculation loop was filled with the precipitated protein. Samples were then collected periodically from the permeate and retentate outlets. The precipitated protein was collected by centrifugation, redissolved by mixing with 2 M glycine (Sigma-Aldrich, St. Louis, MO) in approximately a 5:1 ratio to lower the pH to <4.5, and the concentration of solubilized IgG measured by absorbance at 280 nm¹⁸.

2.5 | Critical flux experiments

The critical flux for the IgG precipitate in the hollow fiber module was evaluated using the flux-stepping procedure described previously by Li and Zydney.²⁴ The critical flux experiments were typically performed in total recycle mode, with the retentate and permeate outflow recycled back to the feed reservoir to reduce the amount of required protein. The TMP was evaluated as a function of time at constant values of the filtrate flux, with the flux increased stepwise every 25 min to determine the onset of fouling.

2.6 | Precipitate characterization

The viscosity of the precipitated IgG suspension was evaluated using a capillary viscometer following procedures described by Baek et al.²⁶ and Li and Zydney.²⁴ In each case, the capillary viscometer was first calibrated using DI water.

The particle size distribution was evaluated by laser diffraction using a Mastersizer 3000 (Malvern Instruments Inc., Westborough, MA). The sample tank (Hydro SV unit, Malvern Instruments Inc.) was initially

washed with DI water and then filled with buffer containing the same ${\rm ZnCl_2}$ concentration as the precipitate sample to minimize redissolution of the precipitates. Precipitate samples were added to the system by pipetting the precipitates into the sample tank until the desired obscuration was reached (15–20%). The particle size distribution was calculated using Mie scattering theory, with the refractive index for the protein precipitates determined by minimizing the sum of the squared residuals between the actual and calculated distributions.

3 | RESULTS AND DISCUSSION

3.1 | Critical flux (no recycle)

Precipitates with IgG concentrations of 5 g/L were generated using the continuous precipitation system shown in Figure 1. The solution became turbid immediately after mixing the IgG stock solution with ZnCl₂, that is, just after the entrance to the first static mixer, reflecting the rapid precipitation kinetics using ZnCl₂ as a cross-linking agent. The precipitation yield was evaluated by measuring the IgG concentration in the supernatant obtained after centrifugation of the precipitated protein. The yield was greater than 99% for all IgG concentrations, with no apparent dependence on the IgG concentration. The collected precipitates were stored at 4° C until use in the critical flux experiments.

Typical data for the critical flux experiments are shown in Figure 3 at two different values of the effective wall shear rate:

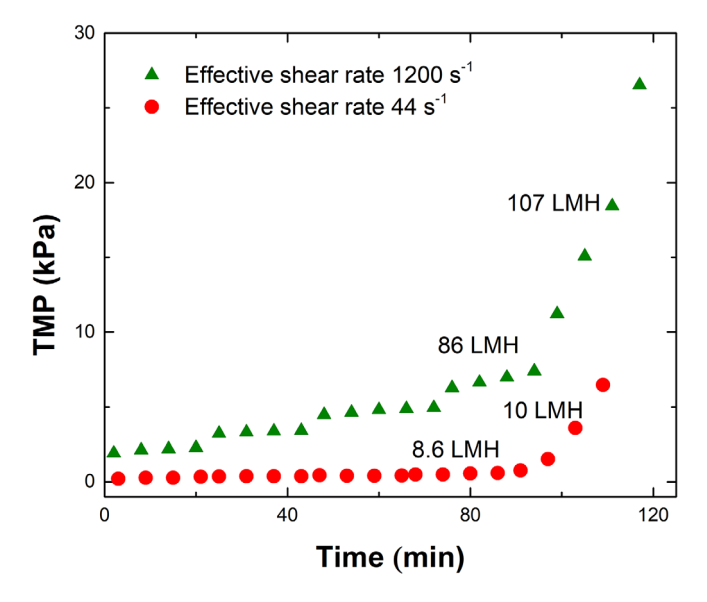


FIGURE 3 Representative data for transmembrane pressure (TMP) as a function of time for two different effective wall shear rates during critical flux experiments with precipitate containing 5 g/L lgG, 10 mM ZnCl₂ and 7 wt% PEG. The pressure values have 95% confidence limits of ± 0.3 kPa and the permeate flux values (in LMH = Lm⁻²h⁻¹) for the intervals below and above the critical flux are labeled immediately above the corresponding TMP data. PEG, polyethylene glycol

$$\gamma_w = \frac{4\bar{Q}}{N\pi R^3},\tag{3}$$

where N and R are the number and inner radius of the hollow fibers. The mean flow rate (\bar{Q}) was determined from the average of the inlet (feed) and outlet (retentate) flow rates. Note that Equation (3) assumes parabolic flow, neglecting any non-Newtonian effects as well as the variation in viscosity with concentration across the concentration polarization boundary layer that may form adjacent to the membrane. In each case, the TMP was evaluated as a function of time (for a minimum of 20 min) at several values of the filtrate flux, until reaching a flux at which there was more than a 60 Pa/min increase in the TMP. This value was chosen since it would extrapolate to a 10 psi increase in TMP during 24 hr of continuous operation (a typical target for continuous bioprocessing). Limited data obtained during continuous operation at a constant flux slightly below the critical flux did show stable TMP for more than 2 hr, which was the longest time that could be explored due to constraints on the available IgG. For the critical flux experiment with an effective shear rate of 44 s⁻¹, the critical flux was greater than 8.6 Lm⁻²h⁻¹, the highest flux at which the TMP remained stable, but below 10 Lm⁻²h⁻¹, which was the first flux at which the TMP showed a clear increase with time during the constant flux filtration. The average of these values (9.3 Lm⁻²h⁻¹) was defined as the critical flux. The critical flux for the experiment at an effective shear rate of 1.200 s⁻¹ was 97 Lm⁻²h⁻¹, which was more than 10x the value at the lower shear rate.

The effect of the wall shear on the critical flux for the IgG precipitates is shown in Figure 4. In each case, the precipitates were formed using 5 g/L IgG in the presence of 10 mM ZnCl₂ and 7 wt% PEG. The critical flux increased with increasing shear rate, with a dependence of approximately $\gamma_w^{0.73}$ as determined from the slope on the log-log plot (evaluated by a simple linear regression fit to the data with R^2 = .99). This dependence on shear rate is greater than the 1/3 power relationship obtained for precipitates of bovine serum albumin (BSA), also formed with ZnCl₂ and PEG; the 1/3 power is consistent with predictions of the classical concentration polarization model based on Brownian diffusion.²⁴

The 0.73 \pm 0.02 power dependence observed in Figure 4 is closer to the linear (first power) dependence on shear rate predicted by the shear-induced diffusion model for particle MF. 27 The different behavior for the IgG and BSA precipitates may be due to the much larger size of the IgG precipitates as determined by laser diffraction (Figure 5). The IgG precipitates show a maximum in the size distribution around 40 μm , with the particle diameter ranging from 4 to 200 μm . In contrast, the peak maximum for the BSA precipitates is less than 4 μm , with the size varying from only 1 to 10 μm . The larger size of the IgG precipitates would enhance the contribution from shear induced diffusion and could also lead to a significant inertial particle migration due to the tangential flow filtration. 28

As discussed previously, effective washing of the precipitated protein requires the use of membrane systems with relatively high conversion, that is, high ratios of the permeate to feed flow rates. If the permeate flux varies with $\gamma_w^{0.73}$, the conversion should be

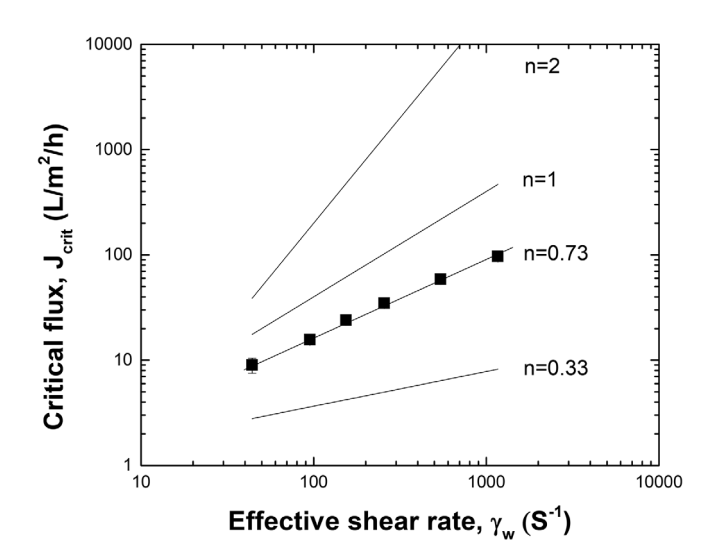


FIGURE 4 Critical flux (accuracy of approximately 1.5 LMH) as a function of the effective wall shear rate for data obtained during microfiltration of IgG precipitates formed using 5 g/L IgG, 10 mM $\rm ZnCl_2$ and 7 wt% PEG. Error bars for the critical flux are smaller than the size of the symbols. Solid lines represent shear rate dependence (slope) of n=0.33 for Brownian diffusion model, n=1 for shear induced diffusion model, and n=2 for inertial lift model. Also shown is linear regression fit to the data on a log-log plot (slope = 0.73). PEG, polyethylene glycol

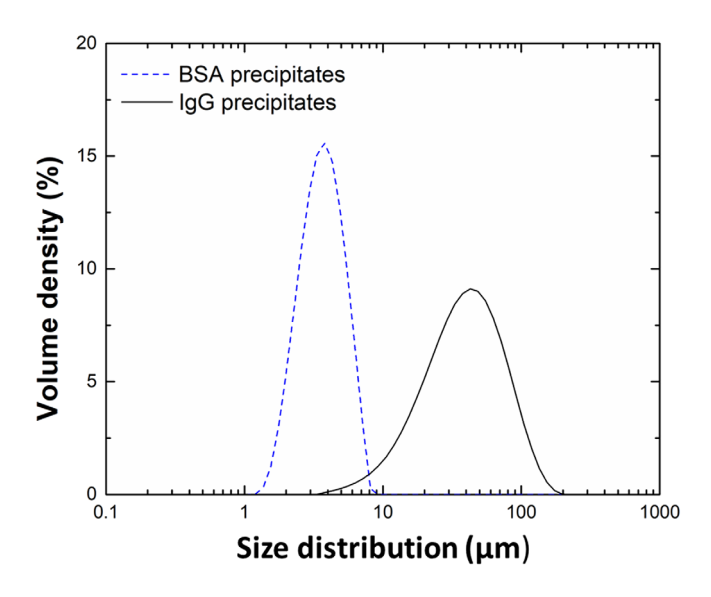


FIGURE 5 Particle size distribution determined by laser diffraction for precipitates formed using BSA and IgG with 5 g/L protein, 10 mM ZnCl $_2$ and 7 wt% PEG. BSA, bovine serum albumin; PEG, polyethylene glycol

proportional to $\gamma_w^{-0.27}$. For the experiments in Figure 4, the maximum conversion was only 65% at the lowest shear rate of $44 \, \text{s}^{-1}$. Extrapolation of this value using the -0.27 power relationship gives a shear rate of $20 \, \text{s}^{-1}$ for 80% conversion. Although it would certainly be possible to operate the hollow fiber module at this low shear rate, the predicted filtrate flux would only be $5.2 \, \text{Lm}^{-2} \text{h}^{-1}$, which would require

the use of very large membrane area modules for large-scale bioprocessing. Even lower shear rates (and filtrate flux) would be required to achieve a conversion of 90%, which is a more likely target to achieve the desired level of HCP removal in bioprocessing applications.

An alternative approach for increasing the conversion in the hollow fiber module is to add a recirculation loop, which can be used to increase the shear rate (and thus the critical flux) while maintaining a constant value of the feed flow rate. However, the use of a recirculation loop will increase the concentration of the precipitate in the hollow fiber module, which could in turn lead to a reduction in the critical flux due to both the increase in suspension viscosity and the potential reduction in back mass transfer between the concentrated solution at the membrane surface and that in the bulk suspension.

3.2 | Effect of IgG concentration

In order to study the effect of the IgG concentration on the critical flux, a series of experiments were performed at a feed flow rate of 5 ml/min, corresponding to an effective wall shear rate of 95 s⁻¹, with the IgG precipitates produced at concentrations of 5, 10, 15, and 25 g/L using the apparatus shown in Figure 1 but with different IgG concentrations in the IgG feed stream: the flow rates and concentrations of all other streams were kept constant. Results are summarized in Figure 6, with the data plotted as a function of the bulk IgG concentration (total amount of IgG in the feed per unit volume). The critical flux decreases with increasing IgG concentration, going from a value of $16 \pm 1 \text{ Lm}^{-2}\text{h}^{-1}$ in the 5 g/L lgG solution to $4.0 \pm 1.4 \text{ Lm}^{-2}\text{h}^{-1}$ in the 25 g/L IgG (where the error limits represent the range between the flux values just above and below the critical flux). The data appear to vary linearly with the IgG concentration over this range of conditions, with linear extrapolation giving a critical flux equal to zero at an IgG concentration of approximately 31 g/L. The physical significance of this "maximum" IgG concentration is unclear since it is certainly possible to generate IgG precipitates at much higher bulk IgG concentrations.

In order to obtain additional insights into the effects of IgG concentration on the critical flux, an independent set of experiments was performed to evaluate the viscosity and the particle size distribution of the IgG precipitates formed at different IgG concentrations. Viscosity data were obtained using a capillary viscometer over a range of pressures (flow rates), with no evidence of any non-Newtonian behavior for shear rates between 500 and $670 \, \text{s}^{-1}$. The viscosity of the MOPS buffer with 10 mM ZnCl₂ and 7% PEG was $1.8 \pm 0.2 \, \text{mPa·s}$ at pH 7 and 20°C (with the error bar representing the 95% confidence interval for multiple repeat measurements). The calculated values of the viscosity (Table 1) increase from 2.1 ± 0.1 to $3.3 \pm 0.2 \, \text{mPa·s}$ as the IgG concentration increases from 10 to $25 \, \text{g/L}$ at constant PEG and ZnCl₂ concentrations, with no evidence of any dramatic increase as the concentration approaches the $31 \, \text{g/L}$ limit seen in Figure 6.

The reduction in critical flux for the IgG precipitates with higher concentration may be due to changes in the size of the IgG

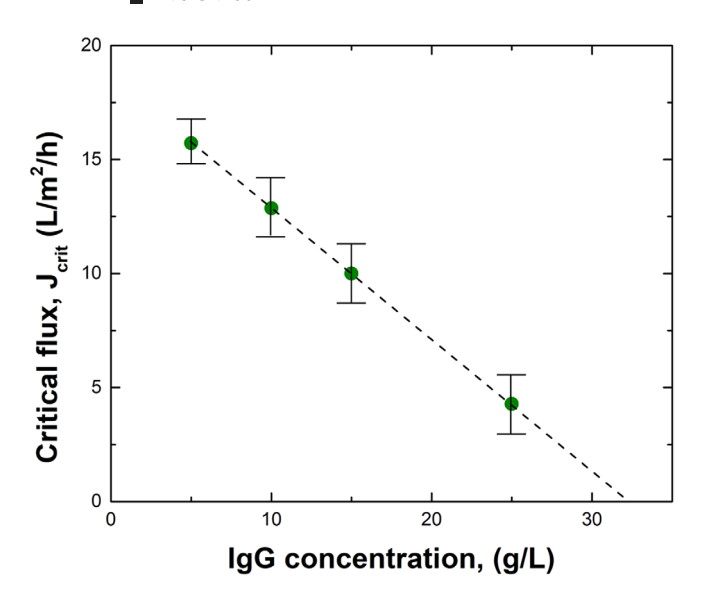


FIGURE 6 Critical flux data as a function of the bulk IgG concentration during microfiltration of IgG precipitates formed with 10 mM ZnCl₂ and 7 wt% PEG at $\gamma_w \approx 95 \text{ s}^{-1}$. Error bars represent the range between the flux values just above and below the critical flux. PEG, polyethylene glycol

TABLE 1 Viscosity of IgG precipitates at different IgG concentrations at neutral pH and 20°C

IgG concentration (g/L)	Viscosity (10 ⁻³ Pa⋅s)
10	2.1 ± 0.1
15	2.6 ± 0.1
25	3.3 ± 0.2

precipitates, which was determined by laser diffraction (Figure 7). The precipitates formed at a concentration of 2.5 g/L lgG show a maximum in the distribution around 20 μm , with the particle diameter ranging from 2 to 50 μm . In contrast, the peak maximum for the 10 g/L precipitates is around 40 μm . The precipitates formed using 25 g/L lgG show a bimodal distribution with peaks at 15 and 85 μm and a diameter varying from 2 to more than 200 μm . These very large precipitates are more than 1/3 the size of the 630 μm inner diameter of the hollow fiber membranes used in the critical flux experiments. Note that the samples in the Mastersizer 3000 had to be diluted around 50 times into a 10 mM ZnCl₂ solution prior to measurement (to achieve the appropriate obscuration range); it is certainly possible that there was some break-up of even larger precipitates during this dilution step.

3.3 | Critical flux correlation

The data for the effects of shear rate and IgG concentration on the critical flux suggest a functional dependence of the following form:

$$J = 0.0217 \gamma_w^{0.73} (31 - C), \tag{4}$$

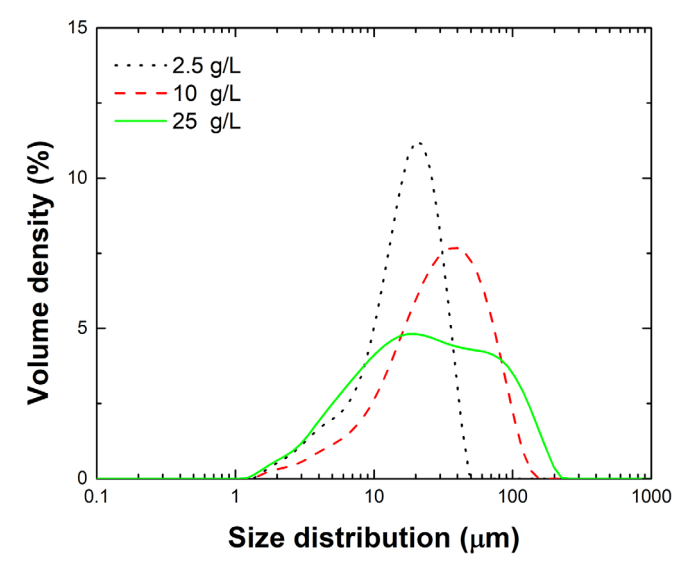


FIGURE 7 Particle size distribution of the precipitates formed at different IgG concentrations with 10 mM ZnCl₂ and 7 wt% PEG. PEG, polyethylene glycol

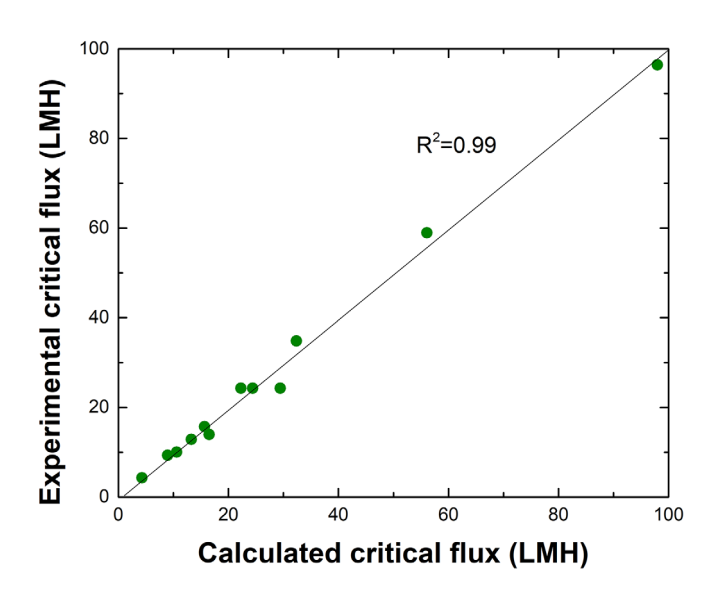


FIGURE 8 Critical flux data obtained over a range of IgG concentrations and shear rates as a function of the model correlation given by Equation (4). Error bars for the experimental flux are smaller than the size of the symbols

where the critical flux is in $Lm^{-2}h^{-1}$, the shear rate is in s^{-1} , and the IgG concentration is in g/L. Critical flux data over a range of conditions (combinations of shear rate and concentration) are shown in Figure 8 in the form given by Equation (4). The data follow the model correlation well, with $R^2 = 0.99$. Critical flux values as high as $97 Lm^{-2}h^{-1}$ were obtained at an effective shear rate of 1,200 s⁻¹ and an IgG concentration of 5 g/L.

The expected conversion (x) in the hollow fiber membrane module can be calculated as:

$$x = \frac{Q_{permeate}}{Q_{feed}} = 5.7 \times 10^{-6} \frac{LN^{0.27}}{R^{1.19}Q_{feed}^{0.27}} \left(1 + \frac{Q_R}{Q_{feed}} - 0.5x\right)^{0.73} (31 - C^*), \tag{5}$$

where L is the fiber length in m, Q_R is the recirculation flow rate in the feed-and-bleed system (in mL/min), and C^* is the IgG concentration at the entrance of the hollow fiber module:

$$C^* = \frac{\frac{C_{feed}Q_R}{1-x} + C_{feed}Q_{feed}}{Q_R + Q_{feed}}$$
 (6)

Equations (5) and (6) are developed assuming steady-state operation with 100% retention of the precipitates; the steady-state approximation is discussed in more detail in the next section. These equations can be solved iteratively to evaluate x as a function of fiber geometry and the feed / retentate flow rates. For a given hollow fiber module, that is, for fixed values of *N*, *R*, and *L*, the conversion will increase as the ratio of the recirculation to feed flow rate increases.

Figure 9 shows experimental data and model calculations for the conversion (x) at different feed concentrations ($C_{\rm feed}$) and feed flow rates ($Q_{\rm feed}$) plotted as a function of the recirculation flow rate. The conversion increases with increasing recirculation rate but approaches an asymptote (x = 0.97 at $C_{\rm feed} = 1$ g/L) at very high recirculation rates, at which point the IgG concentration approaches the maximum value of 31 g/L as given by Equation (5). The maximum conversion decreases with increasing feed IgG concentration. For example, the maximum conversions with the precipitates formed with 3 and 5 g/L IgG concentrations in the feed are only 0.90 and 0.84, respectively.

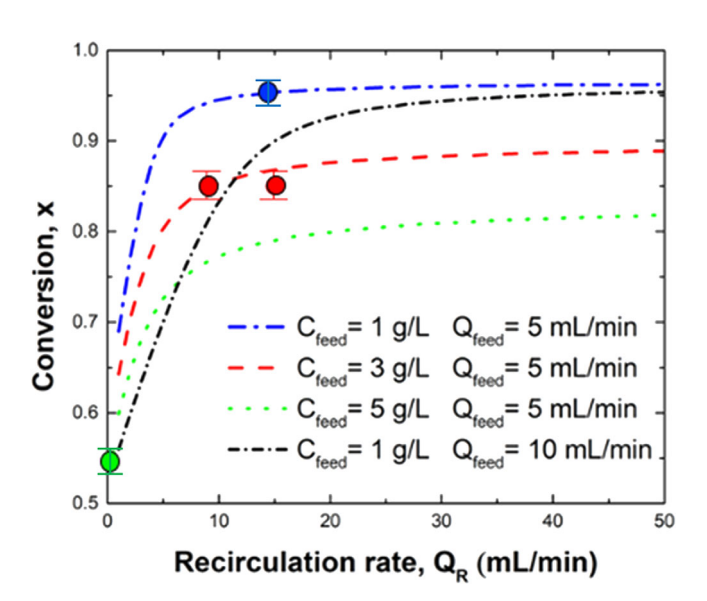


FIGURE 9 Conversion (x) as a function of recirculation rate for a membrane module containing 26 fibers with 0.63 mm ID and membrane area of 105 cm². Filled circles are experimental results with $Q_{feed} = 5$ ml/min and $C_{feed} = 1$ g/L (blue), 3 g/L (red), and 5 g/L (green). Error bars represent the range of conversion between the flux values just above and below the critical flux

The model is in good agreement with limited experimental data obtained using IgG precipitates formed at 1, 3, and 5 g/L with different recirculation rates at a feed flow rate of 5 ml/min.

3.4 | Transient behavior

Although the use of a recirculation loop can provide very high conversions using commercially available hollow fiber modules, one of the potential disadvantages of this approach is that the system can require considerable time to achieve steady-state operation due to the accumulation of retained precipitate in the recirculation loop. A simple mathematical model for the transient behavior was developed by writing a mass balance on the precipitate concentration in the hollow fiber module (including the recirculation loop):

$$V\frac{dC}{dt} = Q_{\text{feed}}[C_{\text{feed}} - (1 - x)C], \tag{7}$$

where C is the average IgG concentration in the hollow fiber module (with total volume V). Note that Equation (7) ignores any loss of IgG precipitate in the permeate. The IgG concentration leaving the module is assumed to be equal to C, i.e., the system is assumed to behave like a continuous stirred-tank reactor (CSTR). Equation (7) can be integrated to give:

$$\frac{C}{C_{\text{feed}}} = \left(\frac{1}{1-x}\right) \left[1 - x \exp\left(\frac{-Q_{\text{feed}}(1-x)t}{V}\right)\right]. \tag{8}$$

Figure 10 shows experimental data for the IgG concentration leaving the hollow fiber module using the feed-and-bleed configuration. The dashed curve is the model prediction given by Equation (8)

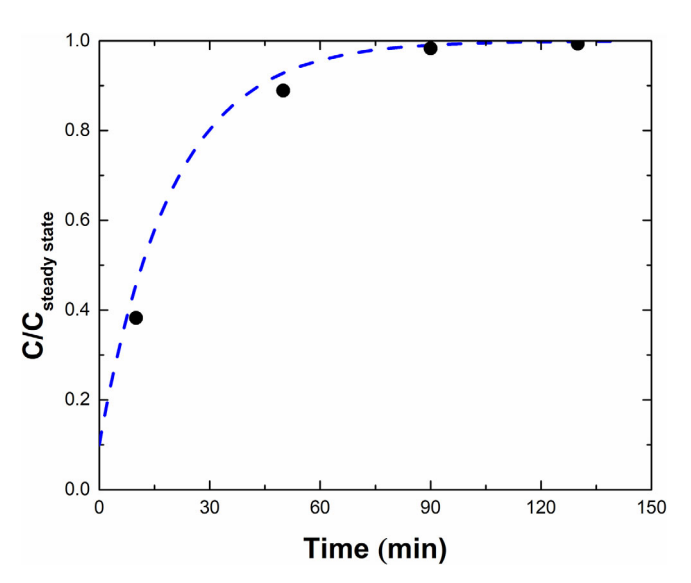


FIGURE 10 The concentration of precipitated IgG in the exit from the hollow fiber module using feed-and-bleed system. Dashed curve is model prediction given by Equation (8)

for V=10.1 ml, $C_{\rm feed}=1.2$ g/L, and $Q_{\rm feed}=5.1$ ml/min. The model is in good agreement with the data indicating that the system can be well described as a stirred tank with uniform concentration. The model predicts that the system reaches within 10% of the steady-state concentration when $t>\frac{2.2V}{Q_{\rm feed}(1-x)}$, which will occur after approximately 50 min for a conversion of x=0.9 and only 25 min for a conversion of 80%. Note that this system takes significantly less time to reach steady state than the 400 min reported by Burgstaller et al. 22 due to the elimination of the large retentate vessel.

Model calculations indicate that conversions greater than 90% can be achieved for a feed with 1.2 g/L IgG concentration at a flow rate of 5 ml/min using a recirculation flow rate of at least 10 ml/min. Figure 11 shows data for the axial pressure drop and TMP as a function of time during operation of the hollow fiber module using a feed-and-bleed configuration with a recirculation rate of 14 ml/min operated at a constant permeate flow rate of 4.5 ml/min to obtain 90% conversion. Both pressure drops increase slowly during the initial 100 min of operation due to the increase in retentate concentration as the precipitates accumulate due to the recirculation loop. The TMP was essentially constant over the last 30 min of operation with an

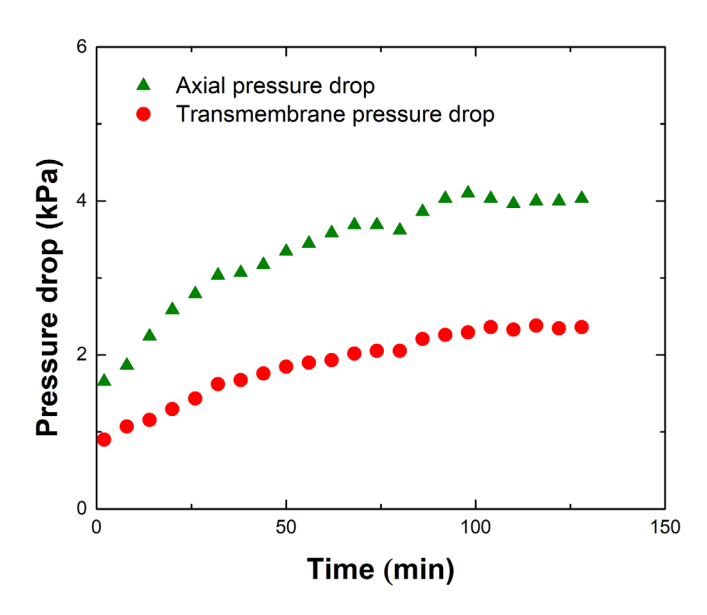


FIGURE 11 Data for the axial and transmembrane pressure drops as a function of time during operation of the hollow fiber module using a 1.2 g/L IgG feed at a flow rate of 5 ml/min in a feed-and-bleed configuration with a recirculation rate of 14 ml/min

increase of less than 1 Pa/min. This would extrapolate to a pressure rise of less than 1.5 kPa (0.2 psi) over 24 hr of operation, suggesting that this hollow fiber module could be used for extended dewatering / washing in a continuous precipitation system. It was not possible to operate the system for longer periods of time due to the large amount of protein that would be required for this type of experiment.

The performance of a continuous precipitation-MF process using a two-stage counter-current washing step¹⁸ with feed-and-bleed operation is examined in Table 2. The feed is assumed to have a mAb concentration of 1 g/L with a flow rate of 5 ml/min (0.3 L/hr); this would correspond to a 10 L perfusion bioreactor operated at 70% volume with one volume exchange per day. The mAb is precipitated using ZnCl₂ and PEG and then concentrated 10-fold using a feed-andbleed MF step with recirculation flow rate of 14 ml/min (0.84 L/hr). Each washing stage uses α = 9 (90% conversion), corresponding to a wash buffer flow rate of 4.5 ml/min (0.27 L/hr). The estimated HCP removal is 910-fold for the combination of the dewatering and washing steps, which is similar to, if not better than, the HCP reduction after a typical platform Protein A chromatography capture step. 11 The capacity of the bench-scale apparatus is 7.2 g mAb/day using the three membrane modules (one for dewatering and two for washing) each with 0.01 m² area. Expected buffer consumption is 0.9 L/g mAb. This is about six times the wash buffer utilized in a typical Protein A chromatography column (0.15 L/g mAb) assuming six column volumes for the wash step and a dynamic binding capacity of 40 g/L. However, it is important to note that the Protein A chromatography step would likely use closer to 0.6 L of total buffer per g mAb after accounting for the elution, stripping, and regeneration steps. The buffer consumption in this system is inversely proportional to the IgG concentration in the feed to the precipitation step. Thus, a precipitate formed from a high titer bioreactor (with 5 g/L mAb concentration) should use less buffer than the Protein A process.

The second row in Table 2 shows the performance of a system designed to process 2000 L of HCCF per day with a mAb titer of $2.5 \, \text{g/L}$, consistent with current perfusion bioreactors operating with one volume exchange per day. In this case, the required recirculation flow rate to give 90% conversion was evaluated by iterative solution of Equations (5) and (6). This system uses relatively small membrane modules (A = $2.8 \, \text{m}^2$ per module) with only $0.36 \, \text{L}$ of buffer per g mAb. The third row shows results from Burgstaller et al. 22 obtained with a mAb (instead of serum IgG). The characteristic time for the system used by Burgstaller et al. 22 (defined as the ratio of the system

TABLE 2 Design calculations for a precipitation-filtration process for mAb purification assuming one volume exchange per day

Scenario	Feed concentration (g/L)	Feed flow rate (L/hr)	Recirculation rate (L/hr)	Characteristic time (min)	Capacity (g mAb / day)	Total membrane area (m²)	Required wash buffer (L/g mAb)	Estimated fold-removal of HCP
7 L perfusion	1	0.3	0.84	2.0	7.2	0.03	0.9	910
2000 L perfusion	2.5	83	430	2.0	5,000	8.4	0.36	910
Burgstaller et al. ²¹	2.5	0.48	24	19	29	0.05	0.36	100
2000 L based on ²¹	2.5	83	4,000	19	5,000	8.6	0.36	100

Abbreviations: HCP, host cell protein; mAb, monoclonal antibody.

9 of 10

hold-up volume to the feed flow rate) was nearly 10x that employed in this work due to the use of a large recycle tank instead of the feed-and-bleed configuration. The fourth row in Table 2 shows the corresponding performance for a 2000 L bioreactor based on the set-up described in Burgstaller et al.²² The recirculation rate (4,000 L/hr) is much higher than that for the scaled process based on the feed-and-bleed configuration examined in this work, while the estimated HCP removal was much smaller due to the use of a single stage washing step.

4 | CONCLUSIONS

Although our previous studies have demonstrated the feasibility of developing a fully integrated continuous process for precipitation, dewatering, washing, and resolubilizing a mAb without any intervening hold steps, the HCP reduction was only 10-fold due to the relatively low conversion (x = 0.6) of the hollow fiber membrane modules. HCP removal levels typical of initial capture chromatography requires conversions of at least 80% and ideally closer to 90%; dewatering followed by a two-stage wash step with 90% conversion can provide nearly 1,000-fold reduction in HCP. In this work, we have demonstrated that such high conversions can be achieved using a feed-and-bleed configuration in which a recirculation loop is used to increase the effective shear rate in the hollow fiber module, thereby increasing the critical flux and in turn the overall conversion.

The design of the feed-and-bleed system is complicated since the recirculation loop increases both the flow rate and the precipitate concentration at the entrance to the module. A simple correlation for the critical flux as a function of shear rate and IgG concentration was developed, allowing rapid identification of experimental conditions that can achieve the targeted conversion.

In addition, the feed-and-bleed system has a relatively slow transient as the IgG concentration builds up in the module. This was modeled using a simple mass balance assuming that the recirculation loop and hollow fiber module act as a CSTR. The resulting model is in good agreement with the experimental data, providing a framework that can be used for the design and controlled operation of the feed-and-bleed configuration.

Design calculations indicate that a continuous precipitation process using a countercurrent 2-stage washing configuration with feedand-bleed operation can achieve more than 900-fold reduction in HCP (including both dewatering and wash stages and assuming no HCP precipitation) with similar buffer requirements as current, typical Protein A capture step. A scaled-up system could process 2000 L of HCCF (equivalent to 5 kg of mAb) per day, consistent with current perfusion bioreactors operating with one volume exchange per day. Future studies will be required to fully demonstrate the potential of this downstream precipitation platform.

ACKNOWLEDGMENTS

This work was supported in part by an NSF GOALI grant CBET 1705642.

CONFLICT OF INTEREST

The authors declare no conflicts of interest.

ORCID

Todd Przybycien https://orcid.org/0000-0003-0111-3640

Andrew L. Zydney https://orcid.org/0000-0003-1865-9156

REFERENCES

- Cohn EJ, Strong LE. Preparation and properties of serum and plasma proteins; a system for the separation into fractions of the protein and lipoprotein components of biological tissues and fluids. J Am Chem Soc. 1946;68(2):459-475. https://doi.org/10.1021/ja01207a034.
- Bertolini J. The purification of plasma proteins for therapeutic use. In: Simon TL, McCullough J, Snyder EL, Solheim BG, G. Strauss R, eds. Rossi's Principles of Transfusion Medicine. Chichester, UK: John Wiley & Sons, Ltd.; 2016:302–320. doi:https://doi.org/10.1002/ 9781119013020.ch27
- Natarajan V, Zydney AL. Protein A chromatography at high titers. Biotechnol Bioeng. 2013;110(9):2445-2451. https://doi.org/10.1002/bit. 24902.
- Somasundaram B, Pleitt K, Shave E, Baker K, Lua LHL. Progression of continuous downstream processing of monoclonal antibodies: current trends and challenges. *Biotechnol Bioeng*. 2018;115(12):2893-2907. https://doi.org/10.1002/bit.26812.
- Tscheliessnig A, Satzer P, Hammerschmidt N, Schulz H, Helk B, Jungbauer A. Ethanol precipitation for purification of recombinant antibodies. *J Biotechnol*. 2014;188:17-28. https://doi.org/10.1016/j. jbiotec.2014.07.436.
- Lohmann LJ, Strube J. Accelerating biologics manufacturing by modeling: process integration of precipitation in mAb downstream processing. *Processes*. 2020;8(1):58. https://doi.org/10.3390/pr8010058.
- Sommer R, Satzer P, Tscheliessnig A, Schulz H, Helk B, Jungbauer A. Combined polyethylene glycol and CaCl₂ precipitation for the capture and purification of recombinant antibodies. *Process Biochem.* 2014;49 (11):2001-2009. https://doi.org/10.1016/j.procbio.2014.07.012.
- Kateja N, Agarwal H, Saraswat A, Bhat M, Rathore AS. Continuous precipitation of process related impurities from clarified cell culture supernatant using a novel coiled flow inversion reactor (CFIR). *Biotechnol J.* 2016;11(10):1320-1331. https://doi.org/10.1002/biot. 201600271.
- Hammerschmidt N, Hobiger S, Jungbauer A. Continuous polyethylene glycol precipitation of recombinant antibodies: sequential precipitation and resolubilization. *Process Biochem.* 2016;51(2):325-332. https://doi.org/10.1016/j.procbio.2015.11.032.
- Jaquez OA, Gronke RS, Przybycien TM. Design of a scalable continuous precipitation process for the high throughput capture and purification of high titer monoclonal antibodies. Presented at: AIChE National Meeting; 2010; https://aiche.confex.com/aiche/2010/webprogram/Paper191335.html.
- Swartz AR, Xu X, Traylor SJ, Li ZJ, Chen W. High-efficiency affinity precipitation of multiple industrial mAbs and Fc-fusion proteins from cell culture harvests using Z-ELP-E2 nanocages. *Biotechnol Bioeng*. 2018;115(8):2039-2047. https://doi.org/10.1002/bit.26717.
- Mullerpatan A, Chandra D, Kane E, Karande P, Cramer S. Purification of proteins using peptide-ELP based affinity precipitation. J Biotechnol. 2020;309:59-67. https://doi.org/10.1016/j.jbiotec. 2019.12.012.
- Haller N, Kulozik U. Separation of whey protein aggregates by means of continuous centrifugation. *Food Bioproc Tech.* 2019;12:1052-1067. https://doi.org/10.1007/s11947-019-02275-1.
- 14. Toro-Sierra J, Tolkach A, Kulozik U. Fractionation of α -lactalbumin and β -lactoglobulin from whey protein isolate using selective thermal

- aggregation, an optimized membrane separation procedure and resolubilization techniques at pilot plant scale. *Food Bioproc Tech*. 2011;6:1032-1043. https://doi.org/10.1007/s11947-011-0732-2.
- Zydney AL. Continuous downstream processing for high value biological products: a review. *Biotechnol Bioeng*. 2016;113(3):465-475. https://doi.org/10.1002/bit.25695.
- Dutta AK, Tran T, Napadensky B, et al. Purification of monoclonal antibodies from clarified cell culture fluid using Protein A capture continuous countercurrent tangential chromatography. *J Biotechnol*. 2015;213:54-64. https://doi.org/10.1016/j.jbiotec.2015.02.026.
- Jabra MG, Yehl CJ, Zydney AL. Multistage continuous countercurrent diafiltration for formulation of monoclonal antibodies. *Biotechnol Prog.* 2019;35(4):e2810. https://doi.org/10.1002/btpr.2810.
- Li Z, Gu Q, Coffman JL, Przybycien T, Zydney AL. Continuous precipitation for monoclonal antibody capture using countercurrent washing by microfiltration. *Biotechnol Prog.* 2019;35(6):e2886. https://doi.org/10.1002/btpr.2886.
- Mondor M, Girard B, Moresoli C. Modeling flux behavior for membrane filtration of apple juice. Food Res Int. 2000;33(7):539-548. https://doi.org/10.1016/S0963-9969(00)00089-2.
- Tanaka Y. Development of a computer simulation program of feedand-bleed ion-exchange membrane electrodialysis for saline water desalination. *Desalination*. 2014;342:126-138. https://doi.org/10. 1016/j.desal.2013.08.016.
- Kim BG, Yoon HJ, Kim SH, Kang HG. Dynamic sequence analysis for feed-and-bleed operation in an OPR1000. Ann Nucl Energy. 2014;71: 361-375. https://doi.org/10.1016/j.anucene.2014.04.014.
- Burgstaller D, Jungbauer A, Satzer P. Continuous integrated antibody precipitation with two-stage tangential flow microfiltration enables constant mass flow. *Biotechnol Bioeng*. 2019;116(5):1053-1065. https://doi.org/10.1002/bit.26922.
- Dutra G, Komuczki D, Jungbauer A, Satzer P. Continuous capture of recombinant antibodies by ZnCl₂ precipitation without polyethylene

- glycol. Eng Life Sci. 2020;20:265-274. https://doi.org/10.1002/elsc. 201900160
- Li Z, Zydney AL. Effect of zinc chloride and PEG concentrations on the critical flux during tangential flow microfiltration of BSA precipitates. *Biotechnol Prog.* 2017;33(6):1561-1567. https://doi.org/10. 1002/btpr.2545.
- Gu Q, Li Z, Coffman JL, Przybycien TM, Zydney AL. High throughput solubility and re-dissolution screening for antibody purification via combined PEG and zinc chloride precipitation. *Biotechnol Prog.* 2020; e3041. https://doi.org/10.1002/btpr.3041.
- Baek Y, Singh N, Arunkumar A, Zydney A. Ultrafiltration behavior of an Fc-fusion protein: filtrate flux data and modeling. *J Memb* Sci. 2017;528:171-177. https://doi.org/10.1016/j.memsci.2017. 01.029.
- Zydney AL, Colton CK. A concentration polarization model for the filtrate flux in crossflow microfiltration of particulate suspensions. *Chem Eng Commun.* 1986;47(1–3):1-21. https://doi.org/10.1080/00986448608911751.
- 28. Belfort G, Davis RH, Zydney AL. The behavior of suspensions and macromolecular solutions in crossflow microfiltration. *J Memb Sci.* 1994;96(1–2):1-58. https://doi.org/10.1016/0376-7388(94) 00119-7.

How to cite this article: Li Z, Chen T-H, Andini E, Coffman JL, Przybycien T, Zydney AL. Enhanced filtration performance using feed-and-bleed configuration for purification of antibody precipitates. *Biotechnol Progress*. 2020;e3082. https://doi.org/10.1002/btpr.3082